Brosinsky, A., Förster, S., Segl, K., Kaufmann, H. (2014): Spectral fingerprinting: sediment source discrimination and contribution modelling of artificial mixtures based on VNIR-SWIR spectral properties. - *Journal of Soils and Sediments*,*14*, 12, pp. 1949—1964.

DOI: http://doi.org/10.1007/s11368-014-0925-1

ANALYSIS AND MODELLING OF SEDIMENT TRANSFER IN MEDITERRANEAN RIVER BASINS

# Spectral fingerprinting: Sediment source discrimination and contribution modelling of artificial mixtures based on VNIR-SWIR spectral properties

**Arlena Brosinsky • Saskia Foerster • Karl Segl • Hermann Kaufmann**

A. Brosinsky (✉)
University of Potsdam, Institute of Earth and Environmental Science, Karl-Liebknecht-Str. 24-25,
14476 Potsdam, Germay
e-mail: arlena.brosinsky@gfz-potsdam.de

A. Brosinsky (✉) • S. Foerster • K. Segl • H. Kaufmann
GFZ German Research Centre for Geosciences, Section 1.4 Remote Sensing, Telegrafenberg, 14473
Potsdam, Germany

(✉) **Corresponding author:**
Arlena Brosinsky,
Tel +49 (0) 331 288 1195
Fax +49 (0) 331 288 1192
e-mail: arlena.brosinsky@gfz-potsdam.de

**Abstract**

Purpose: Knowledge of the origin of suspended sediment is important for improving our understanding of sediment dynamics and thereupon support of sustainable watershed management. An indirect approach to trace the origin of sediments is the fingerprinting technique. It is based on the assumption that potential sediment sources can be discriminated and that the contribution of these sources to the sediment can be determined on the basis of distinctive characteristics (fingerprints). Recent studies indicate that visible–near-infrared (VNIR) and shortwave-infrared (SWIR) reflectance characteristics of soil may be a rapid, inexpensive alternative to traditional fingerprint properties (e.g. geochemistry or mineral magnetism).

Materials and methods: To further explore the applicability of VNIR-SWIR spectral data for sediment tracing purposes, source samples were collected in the Isábena watershed, a 445 km² dryland catchment in the central Spanish Pyrenees. Grab samples of the upper soil layer were collected from the main potential sediment source types along with *in-situ* reflectance spectra. Samples were dried, sieved, and artificial mixtures of known proportions were produced for algorithm validation. Then, spectral readings of potential source and artificial mixture samples were taken in the laboratory. Colour coefficients and physically based parameters were calculated from *in-situ* and laboratory measured spectra. All parameters passing a number of prerequisite tests were subsequently applied in discriminant function analysis for source discrimination and mixing model analyses for source contribution assessment.

Results and discussion: The three source types (i.e. badlands, forest/grassland and an aggregation of other sources, including agricultural land, shrubland, unpaved roads and open slopes) could be reliably identified based on spectral parameters. Laboratory-measured spectral fingerprints permitted the quantification of source contribution to artificial mixtures, and introduction of source heterogeneity into the mixing model decreased accuracies for some source types. Aggregation of source types that could not be discriminated did not improve mixing model results. Despite providing similar discrimination accuracies as laboratory source parameters, *in-situ* derived source information was found to be insufficient for contribution modelling.

Conclusions: The laboratory mixture experiment provides valuable insights into the capabilities and limitations of spectral fingerprint properties. From this study, we conclude that combinations of spectral properties can be used for mixing model analyses of a restricted number of source groups, whereas more straightforward *in-situ* measured source parameters do not seem suitable. However, modelling results based on laboratory parameters also need to be interpreted with care and should not rely on the estimates of mean values only but should consider uncertainty intervals as well.

**Keywords** Artificial mixture • Mixing model • Sediment fingerprinting • Spectroscopy

## 1 Introduction

Suspended sediment entering surface waterways can have a range of negative impacts on water quality, e.g. by eutrophication, increased turbidity, and habitat degradation (cf. review by Owens et al. 2005). Fine sediments were identified as one of the main sources of nonpoint source pollution (Davis and Fox 2009) due to their importance in the transport and storage of nutrients (e.g. phosphorus) and contaminants (e.g. Owens and Walling 2002; Walling 2005). In addition, sediment transported by rivers can adversely affect water quantity due to siltation and thus changes in river morphology or reduction in operational capacities of water supply facilities (e.g. reservoirs) (Owens et al. 2005). Therefore, knowledge of sediment sources is of fundamental importance in understanding complex suspended sediment dynamics and is a prerequisite for sustainable management practices (Walling 2005; Davis and Fox 2009).

Traditional methods of sediment provenance assessment (e.g. erosion mapping, surveying using profilometers or erosion pins, erosion vulnerability indices or erosion plots) are commonly constrained by problems of representativeness and high costs, limiting spatial coverage and monitoring duration of many methods (Peart and Walling 1986; Collins and Walling 2004). Thus, fingerprinting as an alternative indirect measure that has been developed over the past three decades has attracted increasing attention (e.g. Davis and Fox 2009; Collins et al. 2010; Mukundan et al. 2012, Koiter et al. 2013). Sediment fingerprinting usually employs a combination of unique natural tracers (‘fingerprints’) collected from both potential source areas and (suspended) sediment samples that commonly represent mixtures of sources (Walling 2005). It is founded upon two principal assumptions: (1) that the selected fingerprints allow discrimination of potential sources; and (2) that comparison of source and sediment material using these fingerprints permits determination of relative source contribution (Collins and Walling 2004). Thereby, sources are commonly defined either spatially (e.g. tributary sub-catchments, geological sub-areas) or typologically (e.g. land use types, surface vs. sub surface sources) (Collins and Walling 2002).

Investigations have shown that a range of characteristic soil properties can be used as fingerprints to trace back the sources of suspended river sediments, including mineral magnetism (e.g. Yu and Oldfield 1989; Walden et al. 1997), colour (e.g. Grimshaw and Lewin 1980; Krein et al. 2003; Martínez-Carreras et al. 2010a, 2010c), geochemical composition and/or environmental radionuclides (e.g. Motha et al. 2003; Minella et al. 2008; Navratil et al. 2012). Thereby, the use of composite

fingerprints, employing several diagnostic properties, has proven most reliable (e.g. Collins et al. 1997). However, there is no universal recommendation on which properties to include, making parameter retrieval often time-consuming and costly (e.g. Collins and Walling 2002).

Recent investigations have shown that visible (VIS), near-infrared (NIR) and shortwave-infrared (SWIR) diffuse reflectance spectroscopy allow determination of several physical and chemical soil properties (e.g. Kooistra et al. 2003; Viscarra Rossel et al. 2006a, 2006b; Ben-Dor et al. 2009; Richter 2010; Viscarra Rossel and Behrens 2010; Bayer 2013) and that these spectral soil properties can be applied to discriminate and trace-back sediment sources (Martínez-Carreras et al. 2010a, 2010b, 2010c). In addition to being less labor intense than, for example, geochemical analyses, spectroscopy also offers the potential to measure source parameters *in-situ*. Furthermore, it allows measurements of very small amounts of sediment material; for example, Martínez-Carreras et al. (2010a) found 60 mg retained on filters was sufficient to obtain reliable spectral readings, thus enabling inexpensive analyses even of intra-event variability.

In this study, we aim to further assess the potential of this innovative sediment tracing technique, specifically whether:

(1) potential sediment sources can be reliably identified based on VNIR-SWIR spectral features;

(2) spectral fingerprints permit the quantification of source contribution to artificial mixtures; and

(3) field-derived source information (i.e. more rapid) is sufficient for spectral fingerprinting or whether the approach requires laboratory-derived data (i.e. more controlled).

A total of 152 samples of potential sediment sources were collected in the Isábena watershed, a 445 km² dryland catchment in the central Spanish Pyrenees. Spectral reflectance readings were taken in the field as well as in the laboratory from dried and sieved samples using an Analytical Spectral Device (ASD) field spectroradiometer. Then, artificial mixtures of known proportions were produced from dried and sieved samples. Colour coefficients and physically based parameters were calculated from all source and mixture spectra. All parameters passing a number of prerequisite tests were subsequently applied in discriminant function analysis for source discrimination and mixing model analyses for source contribution assessment under controlled conditions.

## 2 Study area

The Isábena catchment (445 km²) is located in the northeast of Spain, in the southern Pyrenees (Fig.

1). The climate of the area can be described as typical Mediterranean mountainous with mean annual temperatures between 9 and 14 °C, and annual precipitation totals of ~770 mm (Verdú 2006). Overall, heterogeneous relief, lithology (Paleogene, Cretaceous, and Quaternary) and land use (agriculture in the valley bottoms, and shrubland, woodland and grasslands in the higher elevations) create a diverse landscape (Müller et al. 2010). The dominance of carbonate rocks and marls in the centre of the catchment lead to the development of badlands, with very high erosion rates and thus are considered to be the major sediment sources (e.g. Fargas et al. 1997; Valero-Garcés et al. 1999; Francke et al. 2008; Alatorre et Beguería 2009).

## 3 Material and methods

### 3.1 Source sampling and data overview

Source material sampling sites were chosen based on previous analyses of land use distribution (Ministerio de Medio Ambiente y Medio Rural y Marino (MARM) 2008), erosion susceptibility (Fargas et al. 1997) and accessibility. Source soil samples were taken during two field campaigns in October 2010 and June 2011, covering the main land use types – shrubland (matorral), woodland, agricultural land and grassland – as well as potential sources, such as badland, unpaved roads and open slopes exposing soil next to roads or channels (Table 1). Sampling sites were chosen in close vicinity (< 100 m) to stream or river reaches to ensure the material will be easily transported to the river. At each site, five grab samples of easily erodible material (top 1-3 cm) were collected from a representative area of approximately 5 m x 5 m. The number of samples collected per land use was approximately proportional to the spatial representation of each source. Sampling locations are shown in Fig. 1.

To verify the assumption of linearly additive behaviour of tracers and to test the performance of the unmixing model, 33 artificial mixtures were produced from up to five source groups in the laboratory. Therefore, known proportions of up to five potential source type samples (forest, agricultural land, shrubland, unpaved road and badland soil material) were mixed in various ratios (5 – 90%).

Suspended sediment samples were collected uisng ISCO automatic samplers at the catchment outlet (44 samples) and near the main subcatchment outlets (46 samples) from September 2011 to June 2012. The sampling procedure is described in detail by Brosinsky et al. (this issue). For this study, sediment material was only used for assumption testing (section 3.4).

### 3.2 Spectral measurements

Spectroscopy can be defined as the study of irradiation as a function of wavelength that is reflected from a surface (Clark 1999). Thereby, a spectrum displaying the quantities of reflected light can be used to identify and characterize material in its quality or quantity (Bayer 2013). Various soil components, such as soil organic carbon content, iron content and texture, exhibit spectral responses in the VIS range of the electromagnetic spectrum (0.4 – 0.7 µm) and thus influence soil colour (Viscarra Rossel et al. 2006a). In addition, some soil constituents produce spectral features in the VIS to SWIR spectral range that can be distinguished by their location in the spectrum and based on parameters describing their shape (Bayer 2013). Mean spectra and the influence of dominant soil constituent are described in Fig. 2.

In this study, an ASD FieldSpec3 High-Res portable spectroradiometer (Analytical Spectral Device Inc., Boulder, Colorado, USA) was used to measure relative reflectance spectra using a white reference (95 % Zenith Alucore Reflectance Target, SphereOptics GmbH, Uhldingen, Germany) as the standard. The ASD spectroradiometer acquires 2150 channels in the 0.35 – 2.5 µm spectral range at a sampling interval of 1.4 nm in the VNIR region (0.35 – 1.0 µm) and 2 nm in the SWIR region (1.0 – 2.5 µm).

Field reflectance spectra of source samples were collected *in-situ* just before grab sampling at the corresponding location using the ASD spectroradiometer with an accessory light source mounted on the light-collecting head of the instrument, thus keeping illumination conditions stable and excluding atmospheric influence for all measurements. Spectral readings were taken at five site-representative locations within 5 m x 5 m where soil was dry and least covered by vegetation/rocks/organic material, and subsequently averaged. The ASD instrument was optimized and white reference readings were taken before every measurement.

For laboratory measurements, source material collected from the five locations per site was thoroughly mixed to provide homogeneous samples. Sediment material was found to be predominantly < 63 µm. Thus, the samples were dry sieved to 63 µm to minimize differences in particle size composition between source and sediment material (Peart and Walling 1986; Smith and Blake 2014). Source material and the 33 artificial mixtures produced from homogenized, sieved source samples were placed in a shallow 5 cm x 5 cm plastic container and oven dried at 60 °C for 24 hours prior to spectral measurements. Spectral readings were taken in a dark room facility using the ASD spectroradiometer

previously used in the field. Illumination was provided by a 2000 W lamp installed at approximately 80 cm from the sample at a zenith angle of 45° and the optical head of the ASD was mounted perpendicular to the sample at a distance of 4 cm, resulting in an effective target area of 1.7 cm. Measurement and instrument conditions were assumed to be constant, however, white reference readings and instrument optimization were performed prior to every measurement. Four readings per sample were taken and subsequently averaged, with the sample rotated 90° after every reading to reduce illumination effects.

### 3.3 Preprocessing of the spectra and parameter calculation

Mean spectra were calculated for each sample and detector jumps at 1.0 and 1.83 µm that occurred on rare occasions were corrected by adaptation to the first detector. All spectra were then smoothed using a Savitzky-Golay filter (Savitzky and Golay 1964) with a Kernel size of 7, meaning that smoothing was applied over seven adjacent spectral channels.

The spectra were averaged to Landsat RGB bands (blue, green and red, 0.45 – 0.52 µm, 0.52 – 0.6 µm, and 0.63 – 0.69 µm, respectively) and multiplied by 255 to get 8-bit colour encoding (Viscarra Rossel et al. 2006a). The derived RGB values were then transformed to eight other colour space models (i.e. Munsell HVC, decorrelated RGB, CIE xyY, CIE XYZ, CIELAB, CIELUV, CIELHC and Helmholtz chromaticity coordinates) using ColoSol software developed by Viscarra Rossel et al. (2006a). The colour gamut of the RGB system forms a cube comprising orthogonal red (R), green (G) and blue (B) axes. Every colour can be produced by a mixture of these three primary colours and represented by a coordinate on or in the cube. The Munsell HVC system commonly used in soil science describes the soil colour qualitatively by the use of hue (H), value (V) and chroma (C) that can be expressed on a numerical scale. Viscarra Rossel et al. (2006a) refer to the decorrelated RGB as a transformation of highly correlated RGB values into three statistically independent components. The CIE models were proposed by the Commission Internationale de l'Eclairage (CIE) (1931) to standardize colour models and facilitate visualization. In the XYZ system introduced first, Y represents brightness while X and Z are virtual components of the primary spectra. Since visualization of these values was difficult, the CIE xyY system was introduced, where Y represents luminance and x and y represent colour variations from blue to red and blue to green, respectively. The CIELAB and CIELUV models were introduced subsequently as an attempt to overcome the non-linearity of the two previous

colour models; L represents brightness or luminance, and a* and b* and u* and v* represent chromaticity coordinates as opponent red–green and blue–yellow scales. The CIELHC model represents a transformation of the CIELAB spherical colour space into cylindrical coordinates, resulting in CIE hue (h*) and chroma (c*) values. Helmholtz chromaticity coordinates describe luminescence (L), dominant wavelength ($\lambda_d$), and purity of excication ($P_e$). All transformation algorithms are described in detail by Viscarra Rossel et al. (2006a) and details of colour models are explained by Wyszecki and Stiles (1982). A summary of the colour parameters applied in this study can be found in Table 2.

Visual inspection of source spectra, laboratory analyses and preceding studies of the catchment area (e.g. Valero-Garcés et al. 1999) suggest that the occurrence of iron oxides, carbonates, organic carbon and different clay minerals differ between various source groups (i.e. land uses). Thus, a set of 77 VNIR and SWIR features found in the literature to be diagnostic of physically based information was calculated following descriptions by Chabrillat et al. (2011) and Bayer et al. (2012). The selected spectral parameters can be divided into spectral indices and three feature types: curve features; hull features; and absorption features. Curve features describe reflectance changes in specific wavelength ranges and were characterized by the mean slope (s) of the spectral curve (Fig. 3a). Hull features describe broader effects on spectra and were characterized by mean slope (s) and reflectance (r) of a convex hull fitted to a defined wavelength range (Fig. 3b). Distinct absorption features were calculated from continuum removed wavelength ranges, i.e. wavelength ranges of which the convex hull was subtracted in order to exclude overall reflectance trends and to allow for intercomparison. Following Bayer at al. (2012), absorption features were analyzed for depth ($d_{max}$) and wavelength ($\lambda_{dmax}$) of maximal absorption, wavelength of maximal absorption according to literature values ($d_{\lambda lit}$), feature width ($w$) as the distance between feature shoulders ($S_{left/right}$), the area between normalized continuum and spectral curve ($A$) and its asymmetry ($AS = A_{left}/A_{right}$) (Fig. 3c). For parameterization of these feature types, reflectance spectra were analyzed for the selected characteristics which were then transformed to numerical parameters. A list of these features can be found in Table 3. Detailed references to previous studies assessing absorption features and their foundations can be found in Bayer et al. (2012).

In total, a set of 98 colour and physical soil reflectance parameters was calculated. Due to similarity of some colour space models and/or calculation of physically based parameters from nearby spectral

244 wavelength, some of these parameters are highly correlated (Viscarra Rossel et al. 2006a; Martínez-
245 Carreras et al. 2010c). However, since colour coefficients may be easily converted and all parameters
246 may potentially be used in spectroscopy and soil science, they will all be considered in the subsequent
247 analyses.
248
249 **3.4 Test of assumptions**
250 Small et al. (2004) summarize a number of principal sources of uncertainty within the established
251 fingerprinting approach. Despite uncertainty in problem formulation (definition of source groups),
252 tracer's discriminating power and source contribution estimation by the use of mixing models, source
253 group variability, analytical errors, and tracer bias, transformation, enrichment and non-linearly additive
254 behaviour may contribute to spurious source quantification results. The potential non-conservative
255 behaviour of tracer properties, with a focus on enrichment and tracer transformation, has recently
256 received attention (Koiter et al. 2013).
257 While some studies have applied particle size and/or organic matter correction mechanisms in model
258 formulation (e.g. Collins et al. 1997; Motha et al. 2003), Smith and Blake (2014) strongly recommend
259 not to use total organic carbon (TOC) correction factors and to carefully consider correcting for particle
260 size since their studies showed that the use of a correction factor may result in large changes in
261 source apportionment or even spurious results. Thus, in this study the problem of size selective
262 transport was addressed by sieving all sampling materials to < 63 µm (e.g. Peart and Walling 1986;
263 Collins and Walling 2002; Walling 2005; Martínez-Carreras et al. 2010a, Smith and Blake 2014).
264 Tracer transformation cannot be excluded either. However, Smith and Blake (2014) recommend to
265 select tracer properties based on knowledge of their geochemical behaviour and to exclude tracers
266 with sediment concentrations lying outside the range of sources. The majority of spectral properties
267 (92 out of 98 for laboratory data and 79 out of 98 for field data) determined from sediment collected at
268 the catchment outlet lie wholly in the range of source materials, indicating that alteration effects may
269 have been relatively small (Walden et al. 1997).
270 Linear additivity of spectral properties was explicitly tested by comparing properties calculated from
271 artificial mixture spectra (described in section 2.2) to properties calculated from mixture spectra that
272 were produced by a linear mixing algorithm using the five source spectra described previously.
273 Spectral parameters were scaled from 0 to 1 and only parameters differing by a root mean square

error (RMSE) of < 0.1 were applied in the tracing procedure (48 out of 92 for laboratory data and 39 out of 79 for field data). Thereby, the number of sources (2 – 5) used to produce the mixture did not seem to have an effect on linearity (results not shown). Following Walling (2005), all remaining parameter values were scaled from 0 to 1 to ensure equal consideration of individual properties in statistical and mixing model analyses, and thus minimize the problem of tracer bias.

Finally, a non-parametric Kruskal-Wallis H-test was conducted, indicating the existence of any interclass contrasts (Collins and Walling 2002). All parameters were able to detect contrasts between the seven source types at the 5 % confidence level.

Thus, in summary, 48 out of 98 parameters calculated from laboratory measured source samples met the prerequisites applied to limit uncertainty to a minimum and were used for subsequent discrimination and unmixing analyses. When tested on field measured source data, an additional seven color parameters and two physically based parameters failed the range tests, resulting in a dataset of 39 parameters. This dataset was used for independent assessment of *in-situ* derived parameters.

### 3.5 Statistical analyses to assess discrimination potential

A Principal Component Analysis (PCA) was performed on the 48 laboratory and 39 *in-situ* parameter sources using The Unscrambler® X 10.2 software (CAMO Software AS., Oslo, Norway). Its major principle can be described as linear transformation of the original data into a new coordinate system, whereas the first coordinate (first principal component (PC)) contains the maximum variability, the second PC (perpendicular to the first PC) contains the maximum share of the remaining variability, and so on. Its major aim is dimension reduction (Reimann et al. 2008). Following Poulenard et al. (2009) the PCA was conducted in order to assess natural clustering of samples and to evaluate overall variability and potential overlap between classes.

Following Collins and Walling (2002) a discriminant function analysis (DFA) was then performed on the two source datasets to test the discriminatory power of (1) individual spectral properties, and (2) a combination of properties drawn by a stepwise selection algorithm. Discriminant function analysis can be used as a classification procedure where a categorical grouping variable known *a priori* is predicted by one or more continuous predictor variables (Reimann et al. 2008). Therefore, it is useful in determining whether a set of variables is effective in discriminating between categories or source

groups. The DFA analyses were performed using R packages (MASS and klaR). Discrimination potential was tested for seven source types (forest, grassland, shrubland, agricultural land, badland, unpaved road, open slopes) and the five source types used for production of mixtures (forest, agricultural land, shrubland, badland, road).

Based on a review of a number of fingerprinting studies, Mukundan et al. (2012) found that most of the investigations were carried out in catchments < 250 km², and concluded that this may represent a threshold at which sediment fingerprinting is feasible. In larger basins (> 500 km²), the expected greater heterogeneity in source type material could exacerbate accurate source determination and thus ascription by increasing intra-class variability. Thus – and since PCA plots and DFA matrices suggest confusion in discrimination between forest and grassland, as well as between shrubland and arable land, road and open slopes – samples of seven source classes were aggregated into three source groups: badland; forest/grassland; and others. Discrimination potential was recalculated for those three source groups using only parameters that passed the Kruskal-Wallis H-test for the defined number of groups (all 48 and 39 parameters for five source groups, and 45 and 39 parameters for three source groups).

### 3.6 Mixing model analyses

Relative contributions of potential sources were estimated by comparing the fingerprint properties of the artificial mixtures with those of the potential sources using a mixing model adapted from other spectroscopic applications. The application of such models is widely adopted in fingerprinting studies (e.g. Yu and Oldfield 1989; Collins et al. 1997; Walden et al. 1997; Motha et al. 2003; Walling 2005; Minella et al. 2008; Martínez-Carreras et al. 2010a, 2010b). Since the model is mathematically over-determined (i.e. has infinite solutions due to the number of tracer properties exceeding the number of potential sources) it must be approximated by minimizing the errors between measured and estimated values. In this study, we used the non-negative least squares algorithm introduced by Lawson and Hanson (1974), where the best approximation is defined as that which minimizes the sum of squared differences between the measured data values and their corresponding modeled values:

$$min\left\| \sum_{i=1}^{n} \left( \sum_{j=1}^{m} a_{ij}\, x_j - b_i \right)^2 \right\} \qquad x_j \geq 0 \qquad \sum_{j=1}^{m} x_j = 1 \qquad \text{Eqn (1)}$$

Where, $a_{i,j}$ is the value of the tracer property $i$ in source type $j$, $x_j$ is the unknown contribution of source type $j$ to the mixture sample, $m$ is the number of source types, $n$ is the number of tracers and $b_i$ is the value of the tracer property in the mixture sample.

Uncertainty associated with modeled contribution results was assessed based on a concept outlined by Beven and Binley (1992) and successfully introduced to fingerprinting studies (e.g. Franks and Rowan 2000; Rowan and Franks 2000; Motha et al. 2003; Small et al. 2004; Martínez-Carreras et al. 2010a). This method attempts to include modeling uncertainty related to source heterogeneity by means of Bayesian modelling. Following Martínez-Carreras et al. (2010a), a Gaussian distribution function was produced from mean and standard deviation calculated from each tracer property per source type. The 100 property values per source group produced this way were limited not to exceed threefold standard deviation (99%) and all values were scaled from 0 to 1 after distribution modelling. This distribution was assumed to approximate its population mean and to represent spatial and temporal tracer variability as well as measurement error.

The model described above was then solved 10,000 times, choosing source information randomly from the Gaussian distributions representing different source groups for each run. Thereby, the model was restricted by the constraints that the source type contributions must all be non-negative and sum to 100%. An additional tolerance criterion was introduced, accepting only those model runs with a RMSE $\leq$ 0.1 between a mixture's measured and its corresponding modelled tracer values. The replicate random sampling permitted the calculation of percentiles, thus providing confidence estimates for the modelled contribution results.

To assess performance of the mixing model using spectral information, it was applied to the 33 artificial mixtures. The contribution of individual source types to the mixture is known and thus allows direct assessment of model performance and potential problems. The model was run therefore using different source type input sets, namely: (a) data from the up to five individual source samples that were used to produce the mixtures (without Monte-Carlo simulation); (b) the mean values calculated from all samples per source type (without Monte-Carlo simulation); and (c) all data simulated for each source type from the Gaussian distribution functions. Input datasets consisted either of a selection of parameters based on stepwise DFA results or combinations of all parameters passing the assumption tests.

## 4 Results

### 4.1 Discrimination potential

Figure 4 shows a two-dimensional scatter plot of scores for the first two principal components (PC1 and PC2) from the PCA performed on source information. These two components summarize most variation in the datasets, where the more similar samples are closer in the plot. Thus, the plots give information on patterns in the samples. No distinct clustering can be observed in Fig. 4 for laboratory and *in-situ* source data. However, the data do group by land use, and is most pronounced for badland and forest soils and soils from arable land (Fig. 4a). Soils sampled from grassland largely overlap with forest samples and shrubland soils overlap with forest/grassland and arable land. Intra-class heterogeneity seems lowest for badland and largest for shrubland and agricultural soils, while unpaved roads and open slopes seem to originate from two separate groups, that in addition overlap with the four other land use groups. These findings are generally very similar for field source data (Fig. 4b).

The first two component plots show a large portion of the information in the data (sum of explained variance 72-82 %), so the relationships can be interpreted with a high degree of certainty. Seven PCs explain 98% of the variance. On the other hand, Walden et al. (1997) conclude that very high explained variance in the first two components may result from low dimensionality of (mineral magnetic) datasets and suggest that only a small number (three to four) source types should be used for realistic source modeling.

Discriminant function analysis was used to assess the percentage of source material samples correctly classified by individual spectral properties that passed the assumption tests. For laboratory measured parameters, the accuracy varied between 20 – 45 % for seven source classes, 30 – 59 % for five source classes and 59 – 77 % for the aggregated three source classes. Hence, the performance of colour parameters and physically based parameters was well mixed, meaning that there were colour parameters as well as physically based parameters with high discrimination potential. However, for a higher number of source classes there was a higher number of colour coefficients with high discrimination accuracies, and the best performing parameter was always a colour parameter. No individual parameter successfully discriminated all samples from three, five or seven source classes. For *in-situ* measured parameters, the accuracy was very similar to that achieved using laboratory parameters, namely 24 – 46 % for seven source classes, 31 – 58 % for five

source classes and 59 – 81 % for the aggregated three source classes. Again, there were colour parameters as well as physically based parameters with high discrimination potential. However, although colour parameters were generally among those parameters with a higher discrimination potential, the best performing were always physically based parameters.

A stepwise DFA was also performed to assess the discrimination potential of composite fingerprints. For laboratory source material samples, a combination of six parameters (*y, b*, AF6 A, AF6* $d_{max}$*, AF5* $d_{\lambda lit}$*,HF3 s)* correctly classified 60 % of the samples for seven source classes, a combination of four parameters (*y, X, AF6 A, a**) correctly classified 70 % for five source classes and a combination of five parameters (*X,* $S_{RGB}$*, CIE.H, AF11* $d_{max}$*, ri)* correctly classified 91 % for the aggregated three source classes. For *in-situ* source material samples, a combination of four parameters (*AF6 A, x, AF12 A, CF*) correctly classified 60 % for seven source groups, a combination of three parameters (*AF6 A, AF10* $d_{max}$*, a*)* correctly classified 73 % for five source groups, and a combination of three parameters (*AF10 A, x, AF6* $d_{\lambda lit}$) correctly classified 88 % for the aggregated three source classes. Hence, the performance of laboratory and field composites was very similar. However, although composite fingerprints always included colour and physically based parameters, for laboratory measured source samples colour parameters were always included first, while for *in-situ* samples physically based parameters were always included first. A summary of accuracies achieved and properties selected by stepwise DFA can be found in Table 4; the first two discriminant functions calculated by a DFA from stepwise selected properties for three source classes are depicted in Fig. 5.

**4.2 Mixing model analyses**

Figure 6 shows the results of unmixing the 33 artificial mixtures produced for algorithm validation. Thus Fig. 6a shows the unmixing results based on the five individual source samples used for mixture production (one sample from badland, shrubland, agricultural land, forest, and road). Independent of the number of sources used to produce the mixtures (two to five), estimated contributions are very similar to the known contributions per source type with few exemptions. Errors are mainly < 10 %.

In Fig. 6b and 6c, source variability is introduced by means of Monte Carlo modelling. Instead of just one potential source sample, the modelling algorithm draws source type information from a pool of 100 gauss distributed samples calculated based on all field samples per source type. This methodology is thought to represent uncertainty intervals by providing estimates on the scatter of

mixing model results. However, knowledge of the true contribution of each source reveals that for several source types, mean estimates (including corresponding uncertainty ranges) fail to represent the true contribution correctly. Using gauss distributions of laboratory source information for unmixing, badland sources can be modelled well while low contributions from agricultural land and unpaved road tend to be overestimated, and higher contributions from forest and unpaved roads tend to be underestimated. Shrubland sources cannot be modelled correctly. Using *in-situ* source information, results are similar for agricultural land, forest and unpaved road sources with the addition of higher uncertainty ranges. Shrubland and badland sources cannot be modelled by the use of *in-situ* data. The restriction of fingerprint parameters used for mixing model analyses to those selected by stepwise DFA as generally executed in fingerprinting studies does not improve the results but seems only to increases uncertainty ranges (results not shown).

Aggregation of the five source types used for mixture production to three classes as suggested by PCA and DFA results (badland, forest and agricultural land/unpaved road/shrubland) did not greatly improve mixing model results, as can be seen from Fig. 7. For laboratory source information (Fig. 7a), aggregation negatively affects the estimation of badland sources by introducing a trend to overestimation especially for lower contributions. Forest sources remain overestimated for low contributions and underestimated (though less) for higher contributions, while the aggregated source group is especially underestimated for higher contributions. Thereby, estimated uncertainty ranges are rather low. Using *in-situ* information, none of the three source types can be modelled accurately (Fig. 7b): badland and forest source contributions are largely underestimated for contributions > 20 %, while the contributions of the aggregated source types seem to be estimated randomly.

## 5 Discussion

### 5.1 Discrimination

Although PCA results indicate grouping of source samples by land use, overlapping of certain classes is evident from the PC plot. Source soil samples from the forest and grassland classes seem indistinguishable which may be due to the higher organic carbon content of these two land use types as compared to all other classes. Source soil samples from shrublands were found to overlap especially with the agricultural land and the forest/grassland groups. This is most likely due to shrublands forming succession states between former agricultural areas that are partly reverting to

natural forests after land abandonment (e.g. Lasanta and Vicente-Serrano 2012). In addition, shrublands are very heterogeneous: While some areas are characterized by a variable number of shrubs (mainly Buxus sempervirens, Genista scorpius and Juniperus communis) on otherwise rather bare soil, other areas may be much more grassy (partly used for sheep and goat grazing), or interspersed with trees. Different transition stages are thus found close-by. There is no conclusive explanation for the arrangement of unpaved road, open slope and badland samples in the PCA plot. Though the material is likely to be pedogenically less developed than material from forest, grassland, shrubland or agricultural land, it does not seem to cluster as separate group(s). Only badland samples form a distinct cluster that is distinguishable from most other samples, while unpaved road and open slope samples intermix with samples from other land uses, presumably with lower soil organic carbon contents. Contrary to expectation, there seems to be no influence of bedrock or area of origin on the distribution of road and open slope samples. No explanation was found for the obvious separation of samples collected from open slopes.

Overall, within-group variation is clearly evident while between-group variation of spectral properties may lack some dimensionality. Walden et al. (1997) presume that this “may influence the effectiveness with which certain suspended sediment samples can be unmixed”.

Results obtained by DFA for classification of seven and five source types support the impression of overlapping classes suggested by PCA plots. However, results for three aggregated classes are well within the range of results obtained in other studies. Using colour coefficients from VNIR reflectance spectra in a 247 km² catchment in Luxembourg, Martínez-Carreras et al. (2010c) report percentages of correctly classified samples of 21 - 48 % (four source groups) and 57 - 74 % (two source groups) for individual tracer properties. In the same study, stepwise DFA yielded maximum percentage of 48.7 % (three properties), and 74.3 % (one property), respectively. However, no mixing model analysis was performed based on this property selection. Using geochemical tracers and radionuclides, for example, Collins and Walling (2002) report classification correctness rates of 29 – 87.5 % for individual fingerprint properties and cumulative values of 94 – 100 % for stepwise selected combinations of five to 12 properties (four source types in 63 - 852 km² basins in Zambia and UK). Walling (2005) describes individual 8 – 62 % and cumulative 100 % (seven parameters, four source types), and cumulative 90 % (seven parameters, two source types) based on geochemical and radionuclide analyses for two catchments (258 km² and 3315 km²) in the UK, respectively. Thus, it was

concluded that the source groups should be aggregated and that the cumulative values of 91 % and 88 % achieved by spectral laboratory and *in-situ* parameters, respectively, are sufficient for subsequent mixing model analyses.

**5.2 Model**

The low error rates achieved for contribution assessment using one individual sample per source type suggest that the use of spectral parameters in general is appropriate for mixing model analyses. However, the introduction of source variability by means of Monte Carlo modelling results in a decrease in modelling accuracy. Estimated mean contributions, including estimated uncertainty, were found not to represent true percentages correctly for several source types. This may be due to large intra-class heterogeneity of some source types. As observed from the PCA plots, badland samples seem to be more homogeneous than all other source classes, and badland contribution can be modelled with high accuracies even under the influence of source variability. However, coefficients of variance calculated for each property of each source type revealed no major differences in variability. Overall, uncertainty was found to generally decrease with higher numbers of tracing properties included in the modelling approach, which is consistent with findings of Franks and Rowan (2000) and Martínez-Carreras et al. (2010a).

Again, contrary to expectations, aggregation of the five source types into three classes was found not to greatly improve mixing model results but possibly to even decrease accuracy. With regard to DFA results, this implies that high discrimination potential does not necessarily result in successful mixing model analyses. No conclusive explanation was found for this effect but it may be related to increased intra-class variability of the new, aggregated group. Overall, mixing model results are in the range generally observed in spectral unmixing studies. For example, Somers et al. (2009) report best mixing model accuracies of $R^2$ of 0.35 – 0.94 when including source or endmember (EM) variability, and Bachmann (2007) found average accuracies of $R^2$ of 0.64 - 0.96. In remote sensing, where spectral mixture analyses are commonly applied, results may be confounded due to a number of reasons. Of these, high intra- and low inter-class variability of EM (potential sources) were found to potentially cause high error rates (e.g. Bachmann 2007; Somers et al. 2011), which is suspected to be the main difficulty in this analysis.

The effects described above are comparable for laboratory and *in-situ* measured spectral parameters.

514 However, while discrimination yields similar results, estimates of source contributions based on *in-situ*
515 parameters are less successful than estimates based on parameters calculated from laboratory
516 measured spectra. This is most likely due to the differences in the treatment of *in-situ* measured
517 source and laboratory measured mixture samples. While measurement conditions were kept constant
518 during field sampling (use of artificial light source), other factors such as soil moisture and grain size
519 were subject to variability. Both factors exert a key control and may alter spectral reflectance
520 significantly. In addition, averaged spectral measurements collected from the surface topsoil of five
521 individual locations may differ from spectral measurements taken from a mixture of material collected
522 from the top 1-3 cm of these points and further alter reflectance spectra.
523 Since laboratory analyses for geochemistry or mineral magnetic properties, for example, are much
524 more labour intensive and more expensive than spectral measurements, there are few fingerprinting
525 studies working with artificial mixtures. Results obtained in this study seem to contradict findings by
526 Franks and Rowan (2000), who successfully modelled the contribution of five artificial mixtures
527 consisting of five source types based on major chemical groups. On the contrary, Lees (1997) found
528 that certain source type components, as well as four or more sources or sources with similar
529 characteristics, could not be unmixed successfully using mineral magnetic properties of 78 artificial
530 mixtures. This was attributed to magnetic variability, calibration inaccuracies and complex grain
531 interactions found in mixtures. Reasons for variability other than source type heterogeneity in spectral
532 parameters may include scattering effects of soil particles that can be different in mixtures than in pure
533 components or measurement inaccuracies due to minimal sample inhomogeneities that could not be
534 assessed by averaging of point measurements. Lees (1997) stressed the necessity for such laboratory
535 mixture experiments as they provide estimates of capabilities and limitation of the properties and
536 methods applied.
537 Martínez-Carreras et al. (2010a) found a good consistency between both approaches when comparing
538 suspended sediment source ascriptions based on spectral colour parameters to ascriptions based on
539 classical fingerprinting parameters (geochemistry and radionuclides) for three small catchments. Thus,
540 the difficulties described above may be site-specific problems of the fingerprinting method in general.
541 From this experiment, we conclude that spectral parameters can be used for mixing model analyses of
542 a restricted number of source types (3 to 4), that a higher number of parameters to characterize
543 samples results in lower uncertainty estimates, and, although providing good discrimination potential,

544 *in-situ* measured source parameters do not seem suitable for mixing model analyses. However,
545 modelling results based on laboratory-measured parameters also need to be interpreted with care and
546 should not rely on mean estimates only.
547
548 **6 Conclusions**
549 In this study, we aimed to further assess the potential of spectral parameters as innovative sediment
550 tracing properties, with emphasis on the questions of whether:
551 (1) potential sediment sources can be reliably identified based on VNIR/SWIR spectral features;
552 (2) spectral fingerprints permit the quantification of source contributions to artificial mixtures; and
553 (3) field-derived source information is sufficient for spectral fingerprinting.
554
555 We found that:
556 (1) Three aggregated source types can be reliably identified based on spectral parameters. However,
557 discrimination relies on intra- and inter-source variability, thus these findings may differ when
558 transferred to other catchments and/or other source (type) formulation, as is the case for other
559 fingerprint properties.
560 (2) Spectral fingerprints permit the quantification of source contribution to artificial mixtures, whereas
561 introduction of source heterogeneity decreases modelling accuracies for some source types.
562 Aggregation of source types does not improve mixture modelling results but, however, the results do
563 provide valuable insight on how to interpret sediment source ascriptions, where the true contribution is
564 unknown.
565 (3) Despite providing similar discrimination accuracies as laboratory source parameters, *in-situ* derived
566 source information was found to be insufficient for contribution modelling. This is most likely due to
567 differences in soil moisture and grain size in the field. A similar treatment of source and sediment
568 samples (drying, sieving) seems necessary.
569
570 In summary, spectral measurements provide a rapid, non-destructive and cost efficient means to
571 characterize potential sources and analyze mixture samples qualitatively and, with restrictions,
572 quantitatively. In the future, a combination of spectral with more established properties in composite
573 fingerprints, as suggested by Martínez-Carreras et al. (2010a), might increase the dimensionality of

574 the datasets and thus improve tracing reliability. In addition, inclusion of spectral features with no
575 physical basis but high classification potential that pass the assumptions tests may improve modelling
576 reliability. Furthermore, the efficiency of source ascription based on Partial Least Squares Regression
577 (PLSR) models calibrated on artificial mixtures, as proposed by Poulenard et al. (2009, 2012), Evrard
578 et al. (2013) and Legout et al. (2013), could be tested for VNIR-SWIR spectroscopy.
579
580 **Acknowledgments** This research was carried out within the project “Generation, transport and
581 retention of water and suspended sediments in large dryland catchments: Monitoring and integrated
582 modeling of fluxes and connectivity phenomena” funded by the Deutsche Forschungsgemeinschaft
583 (DFG). The authors would like to thank Arne Brauer, Benjamin Kayatz, Iris Kleine and Charlotte
584 Wilczok from the University of Potsdam for their support of field work and Stefan Lips and Heide
585 Kraudelt for their support of laboratory measurements.
586
587 **References**
588 Alatorre LC, Beguería S (2009) Identification of eroded areas using remote sensing in a badlands
589 landscape on marls. Catena 76:182–190
590 Alatorre LC, Beguería S, García-Ruiz JM (2010) Regional scale modeling of hillslope sediment
591 delivery: A case study in the Barasona Reservoir watershed (Spain) using WATEM/SEDEM. J
592 Hydrol 391:109–123
593 Bachmann M (2007) Automatisierte Ableitung von Bodenbedeckungsgraden durch MESMA-
594 Entmischung. Dissertation, University of Würzburg, Germany
595 Bayer A, Bachmann M, Müller A, Kaufmann H (2012) A comparison of feature-based MLR and PLS
596 regression techniques for the prediction of three soil constituents in a degraded South African
597 ecosystem. Appl Environ Soil Sci
598 Bayer A (2013) Methodological Developments for Mapping Soil Constituents using Imaging
599 Spectroscopy. Dissertation, University of Potsdam, Germany
600 Brosinsky A, Foerster S, Segl K, López-Tarazón JA, Piqué G, Bronstert A (this issue) Spectral
601 fingerprinting: Characterising suspended sediment sources by the use of VNIR-SWIR spectral
602 information. J Soils Sediments (this issue)
603 Ben-Dor E, Chabrillat S, Dematte JAM, Taylor GR, Hill J, Whiting ML, Sommer S (2009) Using

Imaging Spectroscopy to study soil properties. Remote Sens Environ 113:S38-S55

Beven K, Binley A (1992) The future of distributed models: model calibration and uncertainty prediction. Hydrol Process 6:279-298

Chabrillat S, Eisele, A, Guillaso S, Rogaß C, Ben-Dor E, Kaufmann H (2011) HYSOMA: An easy-to-use software interface for soil mapping applications of hyperspectral imagery. 7th EARSeL SIG Imaging Spectroscopy workshop, Edinburgh, Scotland

Commission Internationale de l'Eclairage (CIE) (1931) CIE Proceedings. Cambridge University Press, Cambridge, UK

Clark RN (1999) Chapter 1: Spectroscopy of Rocks and Minerals and Principles of Spectroscopy. In: Rencz A (ed) Remote Sensing for the Earth Sciences, Vol. 3: Manual of Remote Sensing. John Wiley and Sons, New York, USA, pp 3-58

Collins AL, Walling DE, Leeks GJL (1997) Source type ascription for fluvial suspended sediment based on a quantitative composite fingerprinting technique. Catena 29:1-27

Collins AL, Walling DE (2002) Selecting fingerprint properties for discriminating potential suspended sediment sources in river basins. J Hydrol 261:218-244

Collins AL, Walling DE (2004) Documenting catchment suspended sediment sources: problems, approaches and prospects. Prog Phys Geogr 28:159-196

Collins AL, Walling DE, Webb L, King P (2010) Apportioning catchment scale sediment sources using a modified composite fingerprinting technique incorporating property weighting and prior information. Geoderma 155:249-261

Davis CM, Fox JF (2009) Sediment fingerprinting: review of the method and future improvements for allocating nonpoint source pollution. J Environ Eng 135:490-504

Evrard O, Poulenard J, Némery J, Ayrault S, Gratiot N, Duvert C, Prat C, Lefèvre I, Bonté P, Esteves M (2013) Tracing sediment sources in a tropical highland catchment of central Mexico by using conventional and alternative fingerprinting methods. Hydrol Process 27:911-922

Fargas D, Martinez-Casasnovas J, Poch R (1997) Identification of critical sediment source areas at a regional level. Phys Chem Earth 22:355-359

Francke T, López-Tarazón JA, Vericat D, Bronstert A, Batalla RJ (2008) Flood-based analysis of high-magnitude sediment transport using a non-parametric method. Earth Surf Process Landforms 33:2064-2077

634 Franks SW, Rowan JS (2000) Multi-parameter fingerprinting of sediment sources: Uncertainty
635 estimation and tracer selection. In: Bentley LR et al (eds) Computational Methods in Water
636 Resources. Balkema, Rotterdam, The Netherlands, pp 1067-1074
637 Grimshaw DL, Lewin J (1980) Source identification for suspended sediments. J Hydrol 47:151-162
638 Koiter AJ, Owens PN, Petticrew EL, Lobb DA (2013) The bahavioural characteristics of sediment
639 properties and their implications for sediment fingerprinting as an approach for identifying
640 sediment sources in river basins. Earth Sci Reviews 125:24-42
641 Kooistra L, Wanders J, Epema GF, Leuven RSEW, Wehrens R, Buydens LMC (2003) The potential of
642 field spectroscopy for the assessment of sediment properties in river floodplains. Anal Chimi
643 Acta 484:189-200
644 Krein A, Petticrew EL, Udelhoven T (2003) The use of fine sediment fractal dimensions and color to
645 determine sediment sources in a small watershed. Catena 53:165-179
646 Lasanta T, Vicente-Serrano SM (2012) Complex land cover change processes in semiarid
647 Mediterranean regions: An approach using Landsat images in northeast Spain. Remote Sens
648 Environ 124:1-14
649 Lawson CL, Hanson RJ (1974) Solving Least Squares Problems. Englewood Cliffs, Prentice-Hall, 340
650 pp
651 Lees JA (1997) Mineral magnetic properties of mixtures of environmental and synthetic materials:
652 linear additivity and interaction effects. Geophys J Int 131:225-346
653 Legout C, Poulenard J, Nemery J, Navratil O, Grangeon T, Evrard O, Esteves M (2013) Quantifying
654 suspended sediment sources during runoff events in headwater catchments using
655 spectrocolorimetry. J Soils Sediments 13:1478-1492
656 Martínez-Carreras N, Udelhoven T, Krein A, Gallart F, Iffly J, Ziebel J, Hoffmann L, Pfister L, Walling
657 DE (2010a) The use of sediment colour measured by diffuse reflectance spectrometry to
658 determine sediment sources: Application to the Attert river catchment (Luxembourg). J Hydrol
659 382:49-63
660 Martínez-Carreras N, Krein A, Udelhoven T, Gallart F, Iffly JF, Hoffman L, Pfister L, Walling DE (2010b)
661 A rapid spectral-reflectance based fingerprinting approach for documenting suspended
662 sediment sources during storm runoff events. J Soils Sediments 10:400-413
663 Martínez-Carreras N, Krein A, Gallart F, Iffly JF, Pfister L, Hoffmann L, Owens PN (2010c) Assessment

664 of different colour parameters for discriminating potential suspended sediment sources and
665 provenance: A multi-scale study in Luxembourg. Geomorphology 118:118-129
666 Minella JPG, Walling DE, Merten GH (2008) Combining sediment source tracing techniques with
667 traditional monitoring to assess the impact of improved land management on catchment
668 sediment yields. J Hydrol 348:546-563
669 Ministerio de Medio Ambiente y Medio Rural y Marino (MARM) (2008) Mapa de cultivos y
670 aprovechamientos 1:50,000
671 Motha JA, Wallbrink PJ, Hairsine PB, Grayson RB (2003) Determining the sources of suspended
672 sediment in a forested catchment in southeastern Australia. Water Resour Res 39:1056
673 Müller EN, Güntner A, Francke T, Mamede G (2010) Modeling sediment export, retention and reservoir
674 sedimentation in drylands with the WASA-SED model. Geosci Model Dev 3:275–291
675 Mukundan R, Walling DE, Gellis AC, Slattery MC, Radcliffe DE (2012) Sediment source fingerprinting:
676 transforming from a research tool to a management tool. J Amer Water Resour Assoc
677 48:1241-1257
678 Navratil O, Evrard O, Esteves M, Legout C, Ayrault S, Némery J, Mate-Marin A, Ahmadi M, Lefèvre I,
679 Poirel A, Bonté P (2012) Temporal variability of suspended sediment sources in an alpine
680 catchment combining river/rainfall monitoring and sediment fingerprinting. Earth Surf Process
681 Landforms 37:828-846
682 Owens PN, Walling DE (2002) The phosphorus content of fluvial sediment in rural and industrialized
683 river basins. Water Res 36:685–701
684 Owens PN, Batalla RJ, Collins AJ, Gomez B, Hicks DM, Horowitz AJ, Kondolf GM, Marden M, Page
685 MJ, Peacock DH, Petticrew EL, Salomons W, Trustrum NA (2005) Fine-grained sediment in
686 river systems: Environmental significance and management issues. River Res Applications
687 21:693–717
688 Peart MR, Walling DE (1986) Fingerprinting sediment sources: The example of a drainage basin in
689 Devon, UK. In: Hadley RF (ed) Drainage Basin Sediment Delivery. IAHS Publication 159,
690 IAHS Press, Wallingford, UK, pp
691 Poulenard J, Perrette Y, Fanget B, Quetin P, Trevisan D, Dorioz JM (2009) Infrared spectroscopy
692 tracing sediment sources in a small rural watershed (French Alps). Sci Total Environ 407:2808-
693 2819

694 Poulenard J, Legout C, Némery J, Bramorski J, Navratil O, Douchin A, Fanget B, Perrette Y, Evrard O,
695 Esteves M (2012) Tracing sediment sources during floods using Diffuse Reflectance Infrared
696 Fourier Transformed Spectrometry (DRIFTS) A case study in a highly erosive mountainous
697 catchment (Southern French Alps). J Hydrol 414-415:452-462
698 Reimann C, Filzmoser P, Garrett R, Dutter R (2008) Statistical data analysis explained. Applied
699 environmental statistics with R. John Wiley & Sons Ltd., Chichester, UK pp 362
700 Richter N (2010) Pedogenic iron oxide determination of soil surfaces from laboratory spectroscopy
701 and HyMap image data - A case study in Cabo de Gata-Níjar Natural Park, SE Spain.
702 Unpublished Dissertation, Humboldt University Berlin, Germany
703 Rowan JS, Goodwill P, Franks SW (2000) Uncertainty estimation in fingerprinting suspended sediment
704 sources. In: Foster IDL (ed) Tracers in Geomorphology. John Wiley & Sons Ltd., Chichester,
705 UK, pp 279-290
706 Savitzky A, Golay MJ (1964) Smoothing and differentiation of data by simplified least square
707 procedures. Anal Chem 36:1627–1639
708 Small IF, Rowan JS, Franks SW, Wyatt A, Duck RW (2004) Bayesian sediment fingerprinting provides
709 a robust tool for environmental forensic geoscience applications. Geological Society of
710 London, Special Publications, 232:207-213
711 Smith HG, Blake WH (2014) Sediment fingerprinting in agricultural catchments: A critical re-
712 examination of source discrimination and data corrections. Geomorphology 204: 177-191
713 Somers B, Cools K, Delalieux S, Stuckens J, Van der Zande D, Verstraeten W, Coppin P (2009)
714 Nonlinear hyperspectral mixture analysis for tree cover estimates in orchards. Remote Sens
715 Environ 113:1183-1193
716 Somers B, Asner GP, Tits L, Coppin P (2011) Endmember variability in spectral mixture analysis: a
717 review. Remote Sens Environ 115:1603-1616
718 Valero-Garcés BL, Navas A, Machin J, Walling D (1999) Sediment sources and siltation in mountain
719 reservoirs: a case study from the Central Spanish Pyrenees. Geomorphology 28:23-41
720 Verdú JM (2003) Análisis y modelización de la respuesta hidrológica y fluvial de una extensa cuenca
721 de montaña mediterránea (río Isábena, Pre-Pirineo). Unpublished Dissertation, University of
722 Lleida, Spain
723 Viscarra Rossel RA, Minasny B, Roudier P, McBratney AB (2006a) Color space models for soil

724 science. Geoderma 133:320-337
725 Viscarra Rossel RA, Walvoort DJJ, McBratney AB, Janik LJ, Skjemstad JO (2006b) Visible, near
726 infrared, mid infrared or combined diffuse reflectance spectroscopy for simultaneous
727 assessment of various soil properties. Geoderma 131:59-75
728 Viscarra Rossel RA, Behrens T (2010) Using data mining to model and interpret soil diffuse
729 reflectance spectra. Geoderma 158:46-54
730 Walden J, Slattery MC, Burt TP (1997) Use of mineral magnetic measurements to fingerprint
731 suspended sediment sources: approaches and techniques for data analyses. J Hydrol
732 202:353-372
733 Walling DE (2005) Tracing suspended sediment sources in catchments and river systems. Sci Total
734 Environ 344:159-184
735 Wyszecki G, Stiles WS (1982) Color Science: Concepts and Methods, Quantitative data and
736 Formulae. Second Edition, Wiley, New York, USA
737 Yu L, Oldfield F (1989) A multivariate mixing model for identifying sediment source from magnetic
738 measurements. Quaternary Res 32:168-181

## Tables

**Table 1:** Number of samples collected from each potential suspended sediment source by catchment

| | Villacarli | Cabecera | Carrasquero | Con Isábena | Ceguera | Lascuarre | total |
|---|---|---|---|---|---|---|---|
| Agricultural land topsoil | 3 | 1 | 3 | 8 | 4 | 8 | 27 |
| Grassland topsoil | 1 | 10 | 1 | 3 | - | 1 | 16 |
| Shrubland topsoil | 5 | 7 | 4 | 7 | 3 | 10 | 36 |
| Forest topsoil | 4 | 6 | 2 | 7 | 6 | 5 | 30 |
| Badland | 6 | - | 4 | 3 | 1 | - | 14 |
| Open slope | 1 | - | 1 | 5 | 4 | 8 | 19 |
| Unpaved road | 1 | 3 | - | 1 | 2 | 3 | 10 |
| Total | 21 | 27 | 15 | 34 | 20 | 35 | 152 |

**Table 2:** Color parameters derived from different colour space models calculated using ColoSol software (Viscarra Rossel et al. 2006b) [a] marks all parameters that passed prerequisite testing of laboratory measured samples, [b] represents all parameters that passed prerequisite testing of *in-situ* measured samples.

| Colour space model | Parameter | Abbreviation |
|---|---|---|
| Munsell HVC | Hue | $H$ |
| | Value | $V^{a}$ |
| | Chroma | $C^{a,b}$ |
| Decorrelated RGB | Hue | $H_{RGB}{}^{a,b}$ |
| | Light intensity | $I_{RGB}{}^{a}$ |
| | Chromatic information | $S_{RGB}{}^{a,b}$ |
| CIE xyY | Chromatic coordinate x | $x^{a,b}$ |
| | Chromatic coordinate y | $y^{a,b}$ |
| | Brightness | $Y^{a}$ |
| CIE XYZ | Virtual component X | $X^{a}$ |
| | Virtual component Z | $Z^{a}$ |
| CIELUV | Metric lightness function | $L^{a}$ |
| | CC opponent red-green scales | $u^{*a,b}$ |
| | CC opponent blue-yellow scales | $v^{*a,b}$ |
| CIELAB | CC opponent red-green scales | $a^{*a,b}$ |
| | CC opponent blue-yellow scales | $b^{*a,b}$ |
| CIELCH | CIE hue | $CIE.C^{a,b}$ |
| | CIE chroma | $CIE.H^{a,b}$ |
| Helmholtz chromaticity | Dominant wavelength | $\lambda_d\ (nm)^{a,b}$ |
| | Purity of excitation | $P_e{}^{a,b}$ |
| Index | Redness index | $RI^{a}$ |

749 **Table 3:** Physically based spectral features that are calculated for discrimination and unmixing of
750 sediment sources. Feature types that can be ascribed to specific soil constituents may be absorption
751 features (AF), hull features (HF), curve features (CF), or spectral indices. The spectral region
752 describes the wavelength (range) from which the feature was calculated (for AF, the wavelength of $d_{\lambda lit}$
753 is given in brackets, if available). Parameters calculated are given in column parameterization
754 whereas R represents individual wavelength channels used for the calculation of indices and CR
755 represents the continuum removal described in text. The original sources can be found in Chabrillat et
756 al. (2011) and Bayer et al. (2012). [a] marks all parameters that passed prerequisite testing of laboratory
757 measured samples, [b] represents all parameters that passed prerequisite testing of *in-situ* measured
758 samples.

| Soil constituents | Feature type | Spectral region [µm] | Parameterization | Reference |
|---|---|---|---|---|
| Soil organic carbon | AF1 | 1.6-1.815 (1.73) | $d_{max}$, $\lambda_{dmax}$, *w*, *A*, *AS* | Bayer et al. 2012 |
| | AF2 | 2.24-2.41 (2.33) | $d_{max}$, $\lambda_{dmax}$, $d_{\lambda lit}$, *w*, *A*, *AS* | Bayer et al. 2012 |
| | HF1 | 0.45 - 0.74 | **s** [a,b], **r** [a,b] | Bayer et al. 2012 |
| | HF2 | 1.46 - 1.75 | **s** [a,b], **r** [a,b] | Bayer et al. 2012 |
| | SOC1 | 0.4 - 0.7 | **1/(Σ $R_{0.4}$ - $R_{0.799}$ (CR-R))** [a,b] | Chabrillat et al. 2011 |
| | SOC2 | 0.4 - 0.6 | **1/(slope($R_{0.4}$ - $R_{0.6}$)** [a,b] | Chabrillat et al. 2011 |
| | SOC3 | 2.138 - 2.209 | **1/(slope($R_{2.138}$ - $R_{2.209}$)** [a,b] | Chabrillat et al. 2011 |
| Iron | AF3 | 0.45 - 0.68 (0.55) | ***d*max** [a,b], $\lambda_{dmax}$, $d_{\lambda lit}$, *w*, ***A*** [a,b], *AS* | Bayer et al. 2012 |
| | AF4 | 0.58 - 0.8 (0.7) | $d_{max}$, $\lambda_{dmax}$, $d_{\lambda lit}$, *w*, *A*, *AS* | Bayer et al. 2012 |
| | AF5 | 0.75 - 1.3 (0.9) | ***d*max** [a,b], $\lambda_{dmax}$, ***d*λlit** [a,b], *w*, *A*, *AS* | Bayer et al. 2012 |
| | AF11 | 0.45 - 0.63 () | ***d*max** [a,b], $\lambda_{dmax}$, *w*, ***A*** [a,b], *AS* | Chabrillat et al. 2011 |
| | AF12 | 0.75 - 1.04 () | $d_{max}$, $\lambda_{dmax}$, *w*, ***A*** [a,b], *AS* | Chabrillat et al. 2011 |
| | CF | 0.55 - 0.59 | **s** [a,b] | Bayer et al. 2012 |
| | HF3 | 0.45 - 0.75 | **s** [a,b], **r** [a,b] | Bayer et al. 2012 |
| | RI | 0.477 - 0.693 | **$(R_{0.693})^2$/(($R_{0.477}$)*($R_{0.556}$)³)** [a] | Chabrillat et al. 2011 |
| Clay minerals (Al-OH content) | AF6 | 2.1 - 2.29 (2.2) | ***d*max** [a,b], $\lambda_{dmax}$, ***d*λlit** [a,b], *w*, ***A*** [a,b], *AS* | Bayer et al. 2012 |
| | AF7 | 2.27 - 2.41(2.34) | $d_{max}$, $\lambda_{dmax}$, $d_{\lambda lit}$, *w*, *A*, *AS* | Bayer et al. 2012 |
| | AF10 | 2.12 - 2.25 () | ***d*max** [a,b], $\lambda_{dmax}$, *w*, ***A*** [a,b], *AS* | Chabrillat et al. 2011 |
| | HF4 | 0.45 - 0.7 | **s** [a,b], **r** [a,b] | Bayer et al. 2012 |
| | HF5 | 1.46 - 1.75 | **s** [a,b], **r** [a,b] | Bayer et al. 2012 |
| | SWIR FI | 2.209- 2.225 | **$(R_{2.133})^2$/(($R_{2.225}$)*($R_{2.2209}$)³)** [a] | Chabrillat et al. 2011 |
| Carbonate (Mg-OH content) | AF13 | 2.3 - 2.4 () | $d_{max}$, $\lambda_{dmax}$, *w*, *A*, *AS* | Chabrillat et al. 2011 |

759
760
761

762 **Table 4:** Summary of discriminant function analysis (DFA) results for laboratory and *in-situ* samples
763 and discrimination between different numbers of source classes. The DFA accuracy ranges describe
764 the range of accuracies achieved by each individual property, DFA accuracies for stepwise selected
765 property represents the accuracy met by a composition of tracers selected by stepwise DFA. The
766 properties given in brackets are the properties selected by the stepwise algorithm.

| | DFA accuracy ranges | | DFA accuracies for stepwise selected properties | |
|---|---|---|---|---|
| | laboratory | *in-situ* | laboratory | *in-situ* |
| 7 source classes | 20 - 45 % | 24 - 46 % | 60 % *(y, b*, AF6 A, AF6 $d_{max}$, AF5 $d_{\lambda lit}$,HF3 s)* | 60 % *(AF6 A, x, AF12 A, CF)* |
| 5 source classes | 30 - 59 % | 31 - 58 % | 70 % *(y, X, AF6 A, a*)* | 73 % *(AF6 A, AF10 $d_{max}$, a*)* |
| 3 source classes | 59 - 77 % | 59 - 81 % | 91 % *(X, $S_{RGB}$, CIE.H, AF11 $d_{max}$, ri)* | 88 % *(AF10 A, x, AF6 $d_{\lambda lit}$)* |

767
768

769 **Figures**

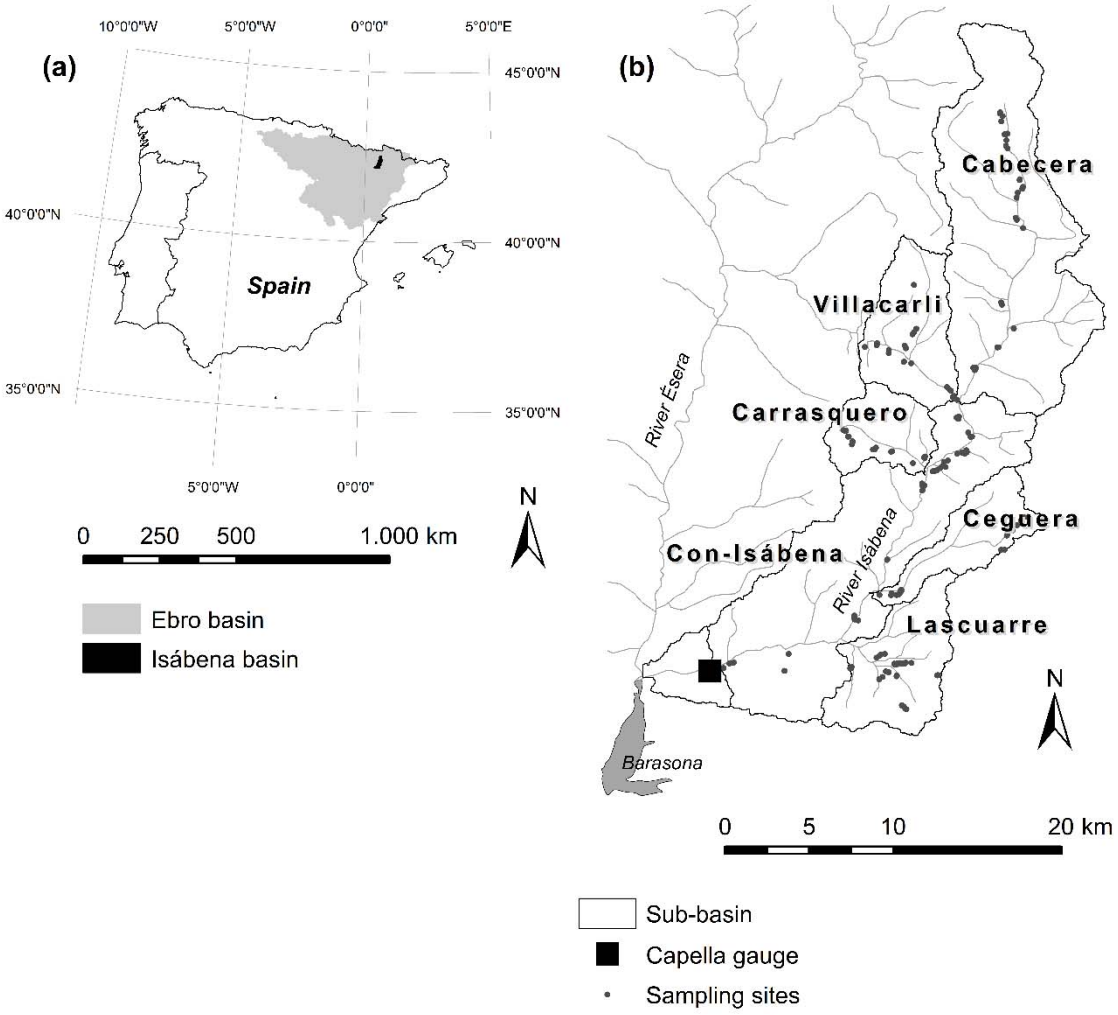


770

771 **Fig. 1:** Overview and location of the Isábena catchment study area (Spain) and sampling sites

772

773

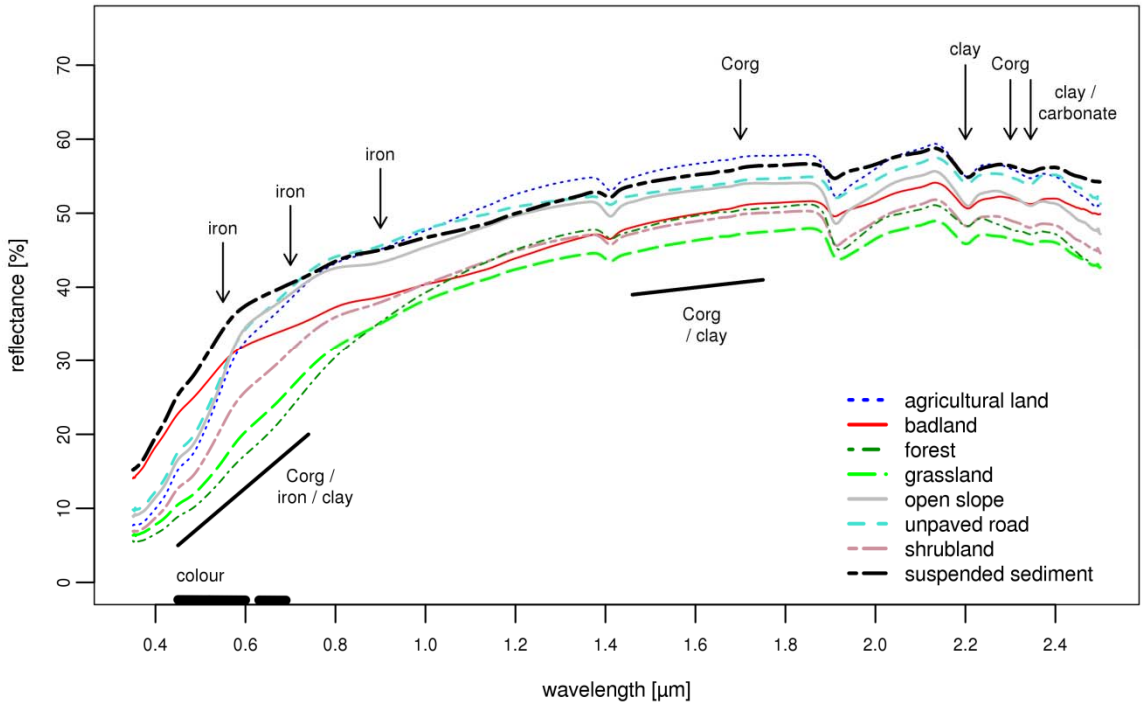


774

775 **Fig. 2:** Average spectra of soils per source type and sediment from the catchment outlet (Capella) and

776 indication of location of features and influencing components (adapted from Bayer et al. 2012)

777

778

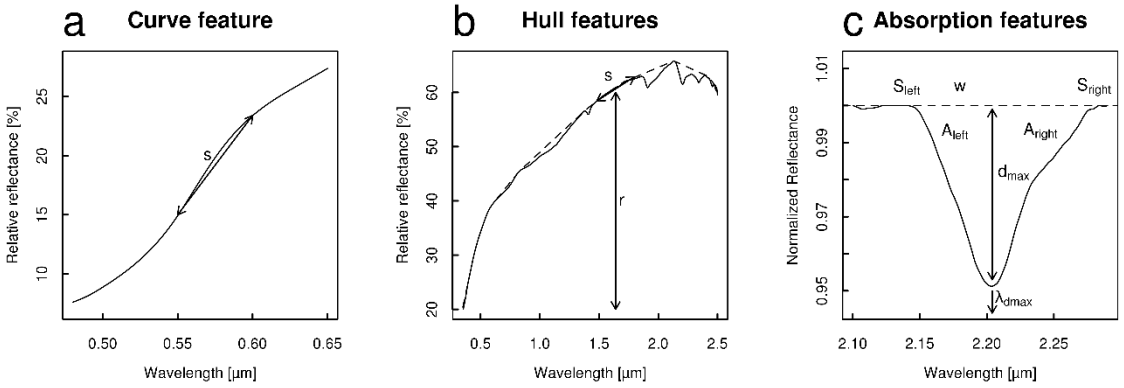


779

780 **Fig. 3:** Parameterization of variables for the spectral features used for the determination of soil organic

781 carbon, iron oxides, clay and carbonate: a) curve features, b) hull features, and c) absorption features.

782 Solid lines represent the reflectance curve and dotted lines represent the continuum of the reflectance

783 curve (adapted from Bayer et al. 2012)

784

785

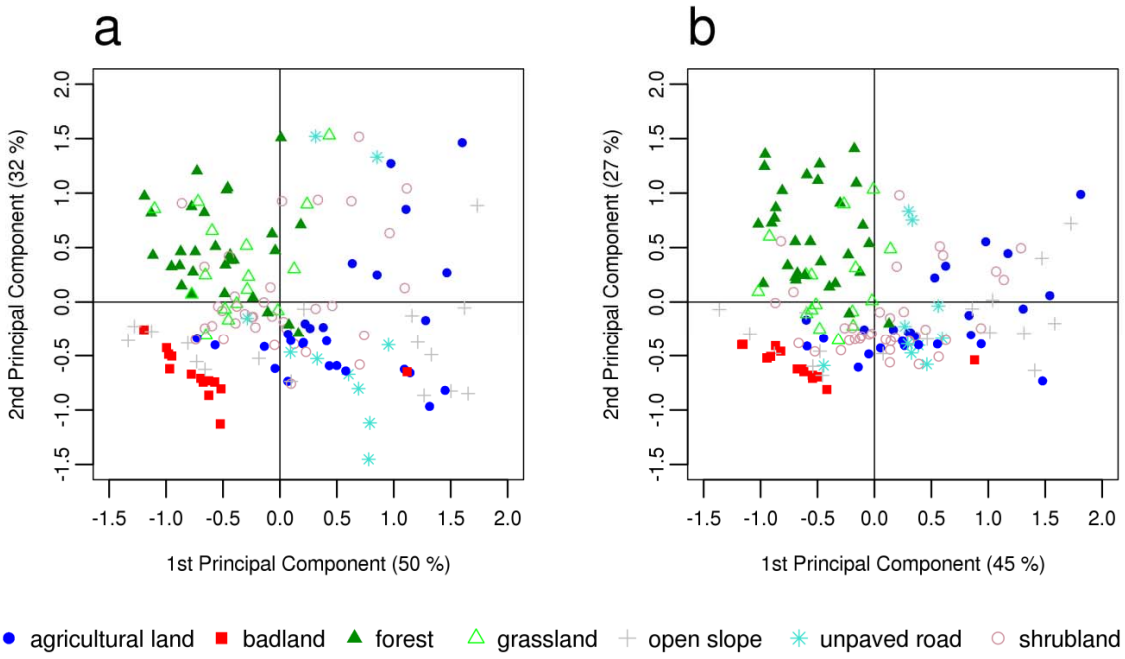


**Fig. 4:** Two-dimensional scatter plot of scores for the first and second principal component (PC) from the principal components analysis (PCA) for: a) laboratory source data by land use; and b) field source data by land use

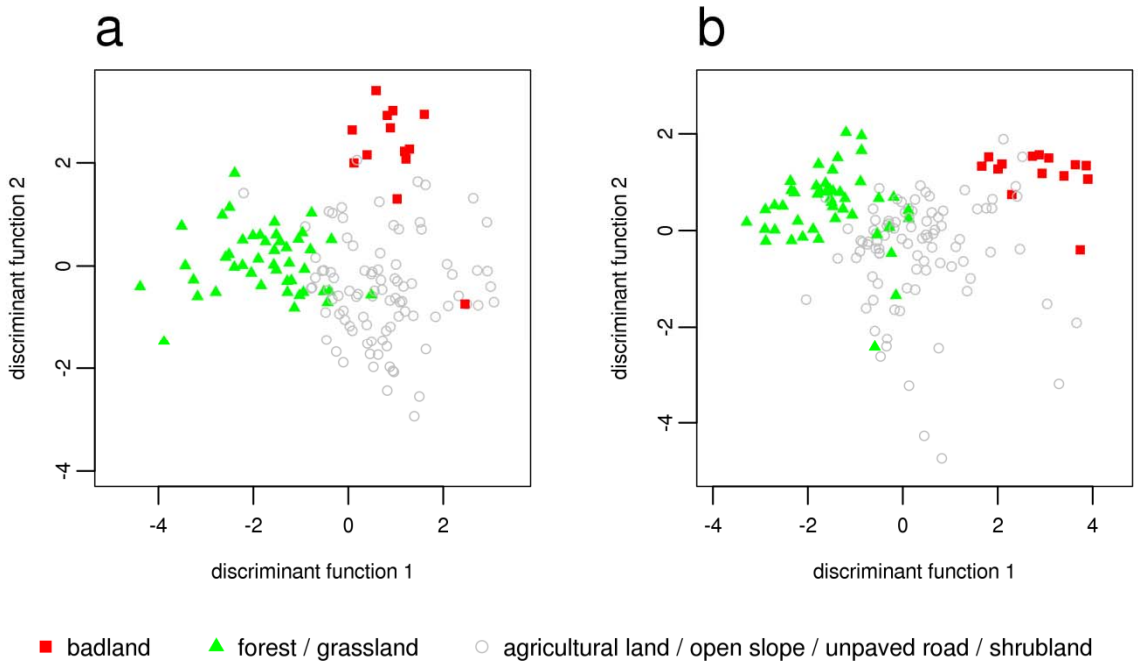


**Fig. 5:** Two-dimensional scatter plot of the first and second discriminant functions from stepwise discriminant function analysis (DFA) with selected parameters for: a) laboratory source data by land use; and b) field source data by land use

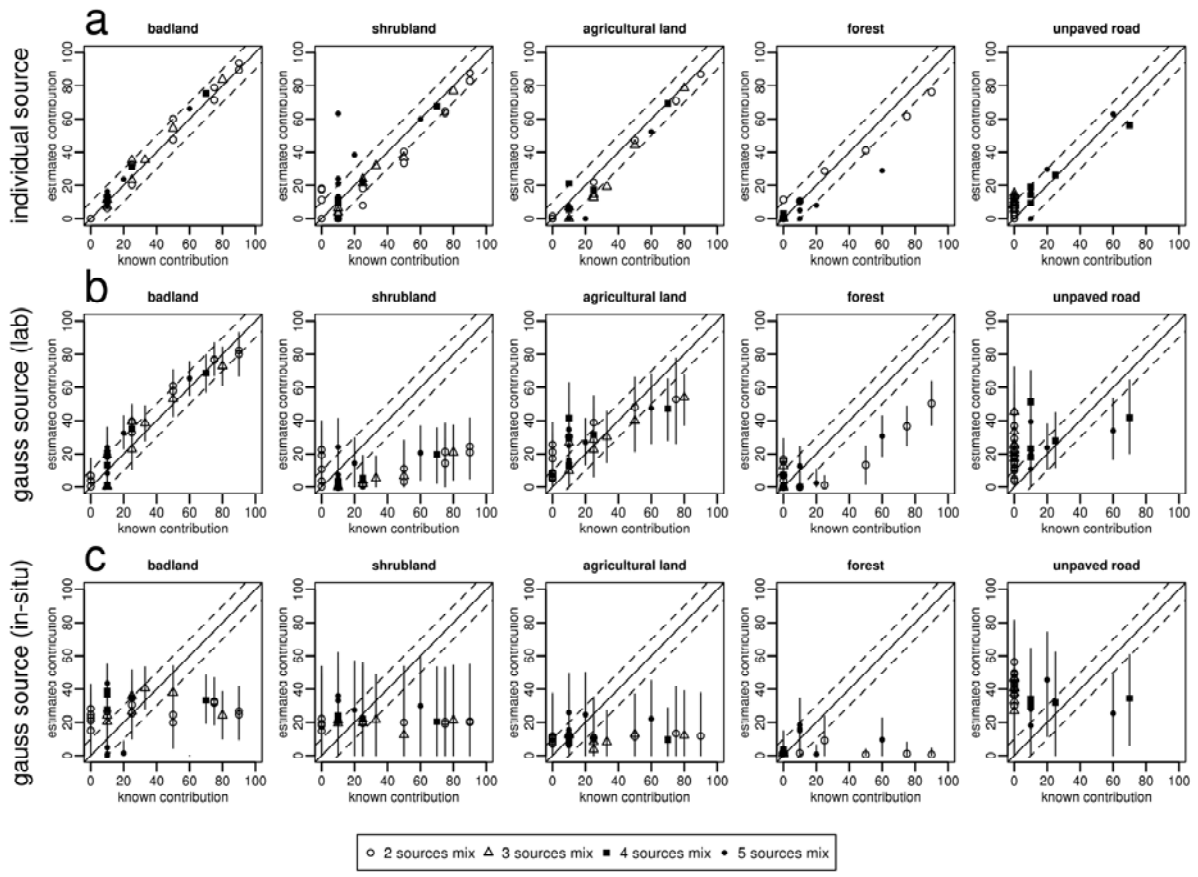


795

796 **Fig.6:** Results of mixing model analyses per source type for the 33 artificial mixtures using all
797 parameters passing the assumption tests: a) based on the five individual source samples used for
798 mixture production; b) based on Gaussian distributed samples calculated from laboratory source
799 information; and c) based on Gaussian distributed samples calculated from *in-situ* information. True
800 contributions per source type are shown on the X, estimated contributions on the Y axes. Symbols
801 represent mean values and error bars represent 90% percentile

802

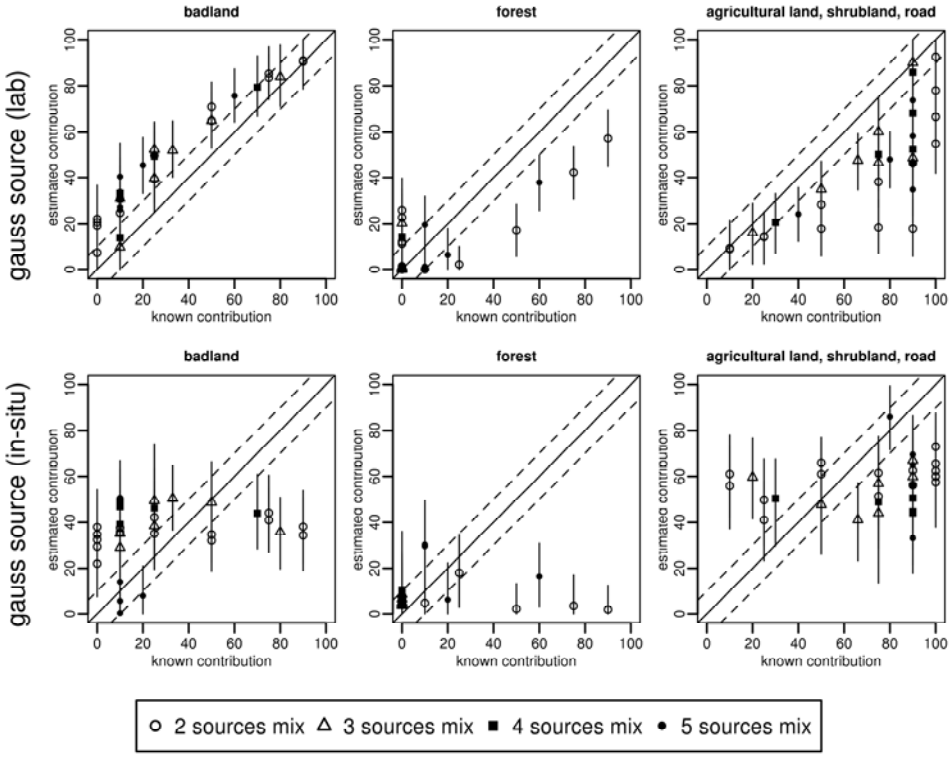


**Fig.7:** Results of mixture modelling per source type for the 33 artificial mixtures produced for algorithm validation aggregated to three source types: a) based on gauss distributed samples calculated from laboratory source information; and b) based on gauss distributed samples calculated from *in-situ* information. True contributions per source type are shown on the X, estimated contributions on the Y axes